Research Article

Environmental Chemistry and Safety
DOI: 10.26599/ECS.2026.9600008
2026, 2, 9600008

Antibiotic and Cu^{2+} Co-Selection in MFCs Treating Swine Wastewater: Antibiotic Resistance Genes Dynamics and Removal Performance

Weidong Shang[1], Yufei Liu[1], Dongle Cheng[1*], Huu Hao Ngo[2], Wenshan Guo[2], Huaqing Liu[1], Lin Li[1], Xinhan Chen[1], and Congcong Liu[1]

[1]Institute of Yellow River Delta Earth Surface Processes and Ecological Integrity, College of Safety and Environment Engineering, Shandong University of Science and Technology, Qingdao 266590, China

[2]Centre for Technology in Water and Wastewater, School of Civil and Environmental Engineering, University of Technology Sydney, Sydney, NWS 2007, Australia

Abstract: Intensive livestock production relies heavily on sulfonamides, quinolones and Cu/Zn additives, creating potent co-selective pressures that accelerate the environmental spread of antibiotic-resistance genes (ARGs). This study examined the effects of combined sulfamethoxazole (SMX), ciprofloxacin (CIP), and copper (Cu^{2+}) in swine wastewater on microbial fuel cell (MFC) performance and ARGs accumulation. Closed-circuit MFCs achieved 95.9% COD removal in pristine influent, 88-90% under antibiotic stress and 81% when Cu^{2+} was present, while maintaining >99% removal of both SMX and CIP via adsorption and biodegradation. Although Cu^{2+} reduced coulombic efficiency by ~30%, stable electricity generation persisted. Cu^{2+} co-stress doubled class 1 integron abundance and tripled sul, qnr, and cus gene copies relative to antibiotic-only conditions. Anodic polarization enriched electroactive and Cu-tolerant taxa (e.g., Trichococcus and Rhodococcus) associated with ARGs, mobile genetic elements, and metal-resistance genes. PICRUSt2 analysis indicated upregulation of DNA repair, metal efflux, and electron-transfer-related pathways, suggesting functional coupling between bioelectrochemical activity and resistance propagation. These findings demonstrate that while MFCs efficiently remove organic matter and antibiotics, they can simultaneously intensify resistance-gene evolution through quantitative, host-associated and functional mechanisms, highlighting the urgent need for post-treatment barriers or operational optimization to curb ARG dissemination from livestock-wastewater treatment systems.

Key words: Microbial fuel cells; antibiotics; Copper ion; antibiotic resistance genes; microbial community

Citation: Shang W D, Liu Y F, Cheng D L, et al. Antibiotic and Cu^{2+} Co-Selection in MFCs Treating Swine Wastewater: Antibiotic Resistance Genes Dynamics and Removal Performance. *Environmental Chemistry and Safety*, 2026, 2, 9600008. https://doi.org/10.26599/ECS.2026.9600008

1. Introduction

The high-density farming environment provides favorable conditions for the outbreak and spread of infectious diseases. Heavy metal elements such as copper (Cu) and zinc (Zn), as well as antibiotics like sulfonamides and quinolones, are widely used in livestock farming [1,2]. These substances play a crucial role in disease prevention and treatment, promoting animal growth, and improving feed utilization efficiency, making them indispensable factors in modern animal husbandry [3-5]. However, due to the low utilization rates of antibiotics and heavy metals in animals, less than 40% of the added amounts actually participate in metabolic processes and exert their intended effects [6,7]. The remaining portions are excreted in their original forms or as metabolites through feces, urine, and wastewater from cleaning pens, ultimately entering aquatic environments. As a result, livestock farming wastewater contains not only nitrogen, phosphorus, and chemical oxygen demand (COD) but also various pollutants such as heavy metals and antibiotics [8,9]. The concentration of SMX and CIP is usually from μg/L to low mg/L, and the concentration of copper (Cu^{2+}) is usually from 0.1 to 5 mg/L, depending on the actual farming conditions [10,11]. Their presence can select for ARGs, and such selection pressure can be substantially intensified by co-existing heavy metals such as Cu^{2+} [1,12]. The co-existence of antibiotics and heavy metals in wastewater can create a complex selective environment that promotes the persistence and dissemination of ARGs, often through the co-selection and mobilization of resistance determinants [13-15].

Microbial fuel cells (MFCs) have emerged as a promising technology for simultaneous wastewater treatment and bioenergy production [16–17]. Previous studies have shown that MFCs can effectively degrade organic pollutants and remove antibiotics from swine wastewater[16,18], with reported removal efficiencies commonly exceeding 80–95% through combined adsorption on anodic biofilms and biodegradation by electroactive microorganisms. These bioelectrochemical conditions provide unique redox environments that can alter microbial metabolism compared with conventional biological treat-

Correspondence to: Cheng D L, dongleleche ng@gmail.com
Received: November 20, 2025; Revised: January 22, 2026; Accepted: January 31, 2026

ment processes [19]. However, the presence of antibiotics and heavy metals in swine wastewater, poses significant challenges to the performance and stability of MFCs. These contaminants can induce the accumulation of ARGs [20–21], which pose a threat to environmental and public health [22]. Accumulating evidence suggests that ARG enrichment in MFCs may be driven by multiple mechanisms, including sustained selective pressure, stimulation of DNA repair and replication pathways, and enhanced horizontal gene transfer mediated by mobile genetic elements [23]. Most existing studies primarily report changes in ARG abundance or community composition, while quantitative comparisons of resistance amplification under single versus combined antibiotic-metal stresses, as well as the identification of specific resistance hosts, remain limited. Moreover, the extent to which bioelectrochemical processes couple microbial metabolic functions with resistance dissemination in MFCs is still poorly understood. Understanding these interactions is crucial for developing effective strategies to mitigate ARG accumulation and enhance the stability and performance of MFCs in treating contaminated wastewater.

Several strategies have been proposed to mitigate ARG risks in bioelectrochemical systems, including post-treatment disinfection, optimization of operational conditions to reduce selective pressure, and integration with downstream treatment barriers. Nevertheless, how combined antibiotic–metal stress influences ARG dynamics and microbial functional potential within MFCs remains insufficiently characterized under realistic livestock-wastewater scenarios [24]. To address this knowledge gap, a comprehensive study was conducted to investigate the effects of SMX, CIP, and Cu^{2+} co-existence in swine wastewater on the accumulation of ARGs in MFCs. Two-chamber MFC reactors were conducted using synthetic swine wastewater spiked with different combinations of SMX, CIP, and Cu^{2+}. The performance of the MFCs in terms of electricity generation, COD removal, antibiotic degradation was evaluated, together with a quantitative comparison of ARG and metal resistance gene amplification under different stress scenarios. Additionally, the microbial community structure was analyzed using 16S rRNA gene sequencing to identify specific taxa potentially responsible for ARG and MRG propagation under bioelectrochemical conditions. The potential functional roles of the microbial communities were further explored using PICRUSt2-based functional prediction to elucidate the coupling between electron transfer–related metabolism and resistance-associated functions. This study aims to provide valuable insights into the complex interactions between microbial communities, electrochemical processes, and contaminant exposure in MFCs, and to highlight the potential of MFCs as a sustainable swine wastewater treatment technology under challenging environmental conditions.

2. Materials and methods

2.1. Construction and operation of the MFC reactors

The two-chamber MFC reactor was made of plexiglass glass. The anode and cathode chamber has a working volume of 294 mL and separated by a proton exchange membrane (PEM) with an effective area of 12.5 cm^2 (radius of 2 cm). The PEM material was immersed in a 4% NaCl solution for 48 hours, during which the solution was replaced three times for pretreatment to remove impurities and expand the membrane surface. The anode was constructed using circular carbon felts with a radius of 2 cm and a thickness of 3 mm, connected by copper wire, while the cathode consisted of a carbon brush with a radius of 2 cm and a length of 5 cm, connected by titanium wire. The anode and cathode were then connected to an external 1000 Ω resistor and data acquisition system using copper wires. The anode and cathode chambers were separated by a proton exchange membrane (PEM) made of Nafion (DuPont, USA) with a thickness of ~180 μm. The inoculum of anode chamber was 200 mL anaerobic sludge, which was taken from anaerobic tank of Nibuwan sewage treatment plant in Qingdao, Shandong Province. Synthetic swine wastewater was used as the influent for the MFC, containing 3.28 g/L glucose, 2.28 g/L $(NH_4)_2SO_4$, 0.44 g/L KH_2PO_4, 0.065 g/L $MgSO_4{\cdot}7H_2O$, and trace metal ions such as Mo, Mn, Ca, Zn, and Co. Additionally, the pH was adjusted to 7.1–7.2. At different specific stages of MFC, the concentration of antibiotics is controlled by directly adding AMX or CIP concentrate to the influent. A peristaltic pump continuously injected the wastewater into the MFC at a constant flow rate of 0.05 mL/min. The MFC reactor was operated at room temperature. Two groups of MFC reactors named open-circuit group (MFC-K), and experimental group (closed-circuit blank group (MFC-0) and closed-circuit experimental group (MFC) were operated simultaneously. Among these reactors, MFC-K was run in an open circuit mode, while MFC-0 and MFC were run in a closed-circuit mode.

After the MFC had stable electricity generation for two weeks, the open-circuit group and experimental group were subjected to experiments under the influent conditions specified in Table S1. Continuous monitoring was conducted to maintain stable operation of the MFC under different conditions. Once the voltage stabilized, experimental data and effluent samples were collected. At the end of each phase, the relative abundance of ARGs was analyzed. Prior to each experiment, the acclimated inoculum was cycled three times to enrich microorganisms on the cathode.

2.2. Analytical methods

After each change in experimental additions, the experimental data and effluent samples were collected after the MFC operating voltage had stabilized for 1 week, and three sets of each water sample were taken in parallel for error comparisons. The COD degradation rate was determined by Fast Digestion-Spectrophotometric method (HJ/T 399-2007). The water samples were filtered through a 0.22 μm filter membrane, and concentrations of SMX and CIP were detected by high-performance liquid chromatography (HPLC) (CTO-20A, SHIMADZU, Japan), the ultraviolet detection wavelength is 257 nm and 278 nm. Antibiotic removal rate (%) is determined based on the concentration difference between the influent and effluent waters. All experimental data are presented as mean ± standard deviation. Statistical differences between two groups were analyzed using Student's t-test, while comparisons among multiple groups were performed using one-way analysis of variance (ANOVA). Differences were considered statistically significant at $p < 0.05$.

2.3. Electricity Generation Performance

The voltage data across the external resistor was recorded

every 30 minutes using a data acquisition system (DAQM-4202C, Zhouzheng). Coulombic efficiency (CE) is a crucial indicator for measuring the efficiency of electron recovery at the anode and can be used to characterize the conversion of organic matter into electrons. The calculation formula is as follows:

$$CE = \frac{8\sum_{i=0}^{t} U_i t_i}{RFV\Delta COD}$$

where U is the output voltage (V), R is the external resistance (1000 Ω), t is the operating time of the reactor per cycle (s), F is the Faraday constant (96,485 C/mol), V is the effective volume of the reactor (0.0003 m^3), and △COD is the amount of COD removed (mg/L).

2.4. DNA extraction and qPCR measurement

At the end of each experimental phase, anode sludge samples were uniformly collected from each reactor. All samples were stored at −20°C prior to DNA extraction. DNA was extracted using a soil kit (DNeasy® PowerSoil® Pro Kit), with detailed methods provided in the supplementary data. A total of 11 target genes were investigated, including sulfonamide resistance genes (*sul-1*, *sul-2*, *sul-3*), ciprofloxacin resistance genes (*qnr-A*, *qnr-S*, *qnr-D*, *aac(6')-ib-cr*), heavy metal resistance genes (*cus-A*, *cop-A*), and mobile genetic elements (MGEs) (*intI-1*). Among these, *sul-1*, *sul-2*, and *sul-3* are commonly found ARGs in nature; *qnr* genes are widely detected in unrelated Enterobacteriaceae species; the protein encoded by *aac(6')-ib-cr* confers resistance to CIP; and *intI-1* indicates horizontal gene transfer. In addition, another method was used to calculate the fold change (FC) of ARGs in effluent samples compared to the initial values [25].

2.5. Illumina sequencing and data analysis

At the end of each experimental phase, sludge from the region near the anode electrode of the MFC was collected and centrifuged at 8000 r/min for 5 minutes. The supernatant was then removed, and the concentrated sludge was stored at −20°C prior to sequencing analysis. The V3-V4 region of the 16S rRNA gene was amplified using polymerase chain reaction (PCR) with the primers 338F (ACTCCTACGGGAGGCAGCAG) and 806R (GGACTACHVGGGTWTCTAAT). High-throughput sequencing results were analyzed on the online platform provided by Shanghai Majorbio Bio-pharm Technology Co., Ltd.

3. Results and discussion

3.1. Performance of MFC for pollutants removal

3.1.1. Performance of COD removal

In the absence of SMX, CIP or Cu^{2+}, the MFC system achieved a high COD removal efficiency of 95.88% (Fig. 1a). Upon exposure to individual antibiotics, the COD removal rates remained relatively stable, with values of 90.46% (SMX) and 90.36% (CIP), indicating that antibiotics alone had a limited impact on organic matter degradation. However, when both antibiotics were present (SC group), the removal efficiency slightly decreased to 88.36%. A more pronounced reduction was observed in the SCC group (81.01%), where Cu^{2+} was introduced alongside the antibiotics. This significant decline is likely attributable to the inhibitory effects of Cu^{2+} on micro-

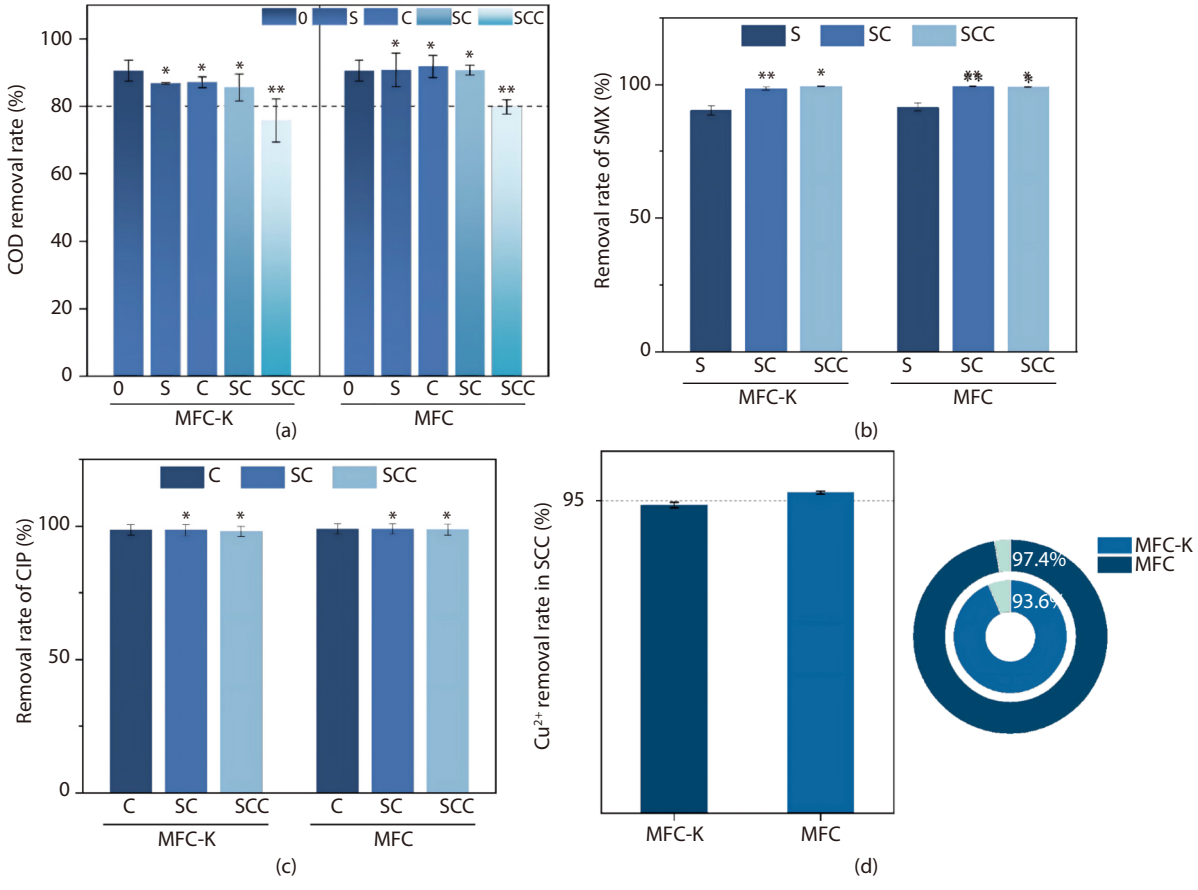

Fig. 1. Removal of COD (a); SMX (b); CIP (c); Cu^{2+} (d) at different stages in MFC-K and MFC. (* p≤0.05 ** p≤0.01 *** p≤0.001)

bial activity, potentially through interference with DNA replication and disruption of cellular metabolic processes. Additionally, the bioaccumulation of Cu^{2+} within bacterial cells may impair their capacity to degrade organic substrates effectively [26–27].

Importantly, under all tested conditions, the closed-circuit MFCs consistently outperformed their open-circuit counterparts, demonstrating higher and more stable COD removal efficiencies. The enhanced COD removal observed under pristine influent conditions can be partially attributed to the stimulatory effect of low doses of Cu^{2+} on microbial metabolism. At environmentally relevant concentrations, Cu^{2+} acts as an essential micronutrient for key oxidoreductases such as cytochrome c oxidase and superoxide dismutase, enhancing respiratory activity and promoting the oxidation of organic matter [28]. This suggests that the electrochemical activity in closed-circuit systems can enhance microbial metabolism and resilience, enabling more effective treatment of complex wastewater containing antibiotics and heavy metals.

Temperature is a key environmental factor affecting microbial metabolism and enzyme activity, and thus COD removal from MFC. COD removal efficiency generally decreases at low temperatures (~18°C in winter) and increases at moderate temperatures (~25°C in summer), with the measured removal efficiency increasing from about 75% in winter to about 80% in summer (Fig. S1). These trends are consistent with the temperature sensitivity of electroactive and heterotrophic microorganisms.

3.1.2. Antibiotic and heavy metal removal

Fig. 1b–d summarise the elimination of SMX (3 mg/L), CIP (3 mg/L) and Cu^{2+} (3 mg/L) across the different experimental phases. SMX removal gradually climbed to 99% as the reactor matured, whereas CIP was consistently degraded at > 95%. The high efficiencies are attributed to the combined effect of (i) rapid adsorption to the anodic biofilm and (ii) subsequent biodegradation by enriched heterotrophs and electro-active taxa [29]. Closed-circuit operation yielded both higher and more stable antibiotic removals than the open-circuit control, evidencing that anodic current stimulates catabolic activity and growth of exoelectrogens such as *Trichococcus*.

The Cu^{2+} removal was also markedly superior in the closed-circuit MFC (Fig. 1d). *Rhodococcus*, a well-documented Cu^{2+} biosorbent [30], dominated the anodic community under moderate metal stress. Biosorption proceeds via electrostatic attraction between the positively charged ion and the deprotonated cell envelope, as well as complexation with surface functional groups. The slightly acidic pH maintained in the anode compartment enhanced the net negative surface charge of *Rhodococcus*, enhancing Cu^{2+} binding [31]. However, during the SCC phase, the relative abundance of *Rhodococcus* declined, most likely because intracellular Cu accumulation damaged cell-wall integrity and reduced specific growth rate. Consequently, absolute Cu^{2+} uptake decreased even though removal efficiency remained > 85%, indicating that biosorption by other taxa and precipitation on the cathode provided supplementary sinks.

The removal of CIP and SMX in the MFC system could be explained by a microbial-mediated transformation process under anaerobic and bioelectrochemical conditions. As shown as Fig. S2-3, the degradation pathway of CIP mainly involved the structural modification and cleavage of piperazine ring, accompanied by deamination, defluorination and decarboxylation, which leads to the instability of the quinolone parent core structure [32]. These transformations reduced the integrity of CIP molecules and generate intermediates with more simplified structures [33]. In the case of SMX (Fig. S4-5), the degradation process was mainly related to the enzymatic ring opening of the isoxazole ring, followed by the progressive conversion of the sulfonamide functional group and possibly a deamination reaction at the aromatic ring. In addition, the breakage of the sulfonamide bond could further produce smaller molecular fragments [34]. The intermediate products formed by both antibiotics can continue to be converted into small molecule compounds suitable for anaerobic microbial metabolism [35]. In addition, degradation intermediates of CIP and SMX were also analyzed for toxicity through T.E.S.T (Fig. S6-7). The intermediates were analyzed at LC50 (mg/L) at 96 h and LC50 (mg/L) at 48 h in M. macrocopa, as well as developmental toxicity and mutagenicity. The toxicity of most intermediates decreased compared with that of CIP and SMX. Although the toxicity of some intermediates increased, the overall toxicity of the solution decreased as the concentration of organic matter decreased during degradation.

3.1.3. Electrical output and coulombic efficiency (CE)

Throughout the continuous-flow experiment, the output voltage was logged every 30 min and used to compute the CE. Fig. 2a presents the steady-state values recorded for the blank (MFC-0) and test (MFC) reactors. It was observed that the CE of the blank control group steadily increased to 11.4% during long-term continuous operation, reflecting biofilm matura-

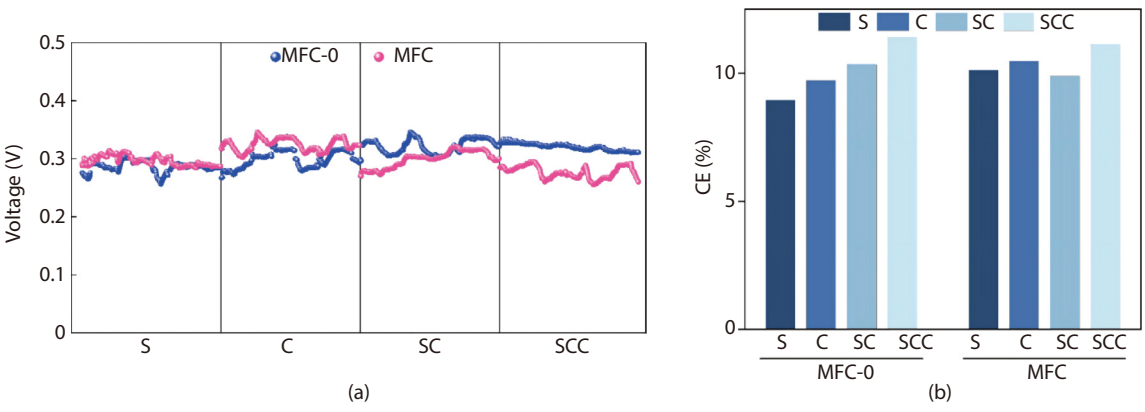

Fig. 2. Voltage profile after stabilization at each stage (a) and Coulomb efficiency (b) .

tion and the selection of electrogenic taxa. To achieve a quantitative comparison of the electrical generation performance under different stress conditions, we determined the power density by calculating the steady-state voltage at each stage [36]. As shown in Fig. S8, the steady-state voltage in the S phase was 0.288 V, corresponding to a power density of about 66 mW m^{-2}. Stage C exhibited higher steady-state voltage (0.324 V) and power density (~84 mW m^{-2}), indicating enhanced electrical generation performance under CIP conditions. The steady-state voltage was slightly reduced to 0.317 V and the power density was about 80 mW m^{-2} in the SC stage. In contrast, upon the addition of Cu^{2+}, the electrogeneration performance was significantly suppressed, with the steady-state voltage decreasing to 0.271 V and the power density decreasing to ~58 mW m^{-2}. Compared with the previous MFC studies for the treatment of antibiotic-and/or copus-containing wastewater, the electrogeneration performance of this study was within the typical range of the two-chamber air cathode MFC, while clearly revealing the inhibition effect of Cu^{2+} co-stress on anode electron transport (Table.S2).

A stable anode potential enriched *Proteobacteria* and *Firmicutes*, populations known for extracellular electron transfer (EET), while non-electrogenic competitors were gradually washed out. When either SMX or CIP was supplied individually, the relative abundance of *Trichococcus*—a recognised exoelectrogen —rose markedly. Its ability to channel carbohydrate oxidation into current generation conferred a selective advantage, allowing it to out-compete fermenters for glucose. Conversely, *Bacteroidetes_vadinHA17*, another EET-capable genus but specialised in protein/amino-acid degradation [37], showed no comparable increase because glucose was the dominant electron donor in the synthetic wastewater.

Addition of Cu^{2+} altered the anode potential and suppressed acidification kinetics, reducing CE by ~30% (Fig. 2b). Consistent with the electrochemical properties, a slight decrease in effluent pH was observed at the SC and SCC stages. This pH change can be attributed to enhanced proton generation associated with anodization of organic substrates and accumulation of organic acids under antibiotic-metal co-stress. However, the wastewater pH remained close to neutral (6.6-7.0), indicating that the MFC system maintained adequate buffering capacity and operational stability. Intracellular Cu accumulation disrupts respiratory enzymes and decreases substrate turnover rates [38], illustrating the tight linkage between metal speciation, microbial metabolism and electrochemical performance. These observations underscore that heavy-metal stress can simultaneously modify surface redox chemistry and inhibit the physiological activity of electrogenic bacteria, leading to lower current recovery and slower organic-matter conversion.

Based on the steady-state electricity generation performance, we conducted a preliminary economic evaluation of the proposed MFC system. Based on an effective reactor volume of 200 mL and a single-stage operation time of 7 days, the energy recovery per unit volume estimated from steady-state voltage was 61.7-88.2 Wh m^{-3} in different operation stages (Table S3). Although the current energy recovered is not sufficient to fully offset the construction cost of the reactor, the use of air cathodes and carbon-based electrodes without noble metal ORR catalysis significantly reduces material and operating costs, and avoids the additional energy consumption required for mechanical aeration. Therefore, the economic advantages of this MFC are more reflected in the system robustness and operation simplicity, rather than the pure pursuit of energy maximization. In the future, it is still necessary to further improve the engineering economy by improving the power density and long-term stability.

3.2. Changes in microbial community structure

3.2.1. Phylum-level community dynamics

16S rRNA profiling revealed that >70% of all sequences in closed-circuit MFCs belonged to six dominant phyla: *Firmicutes*, *Proteobacteria*, *Bacteroidota*, *Actinobacteriota*, *Chloroflexi* and *Synergistota* (Fig. 3a). The first three are well-established electrogenic taxa [39–40]. *Firmicutes* secrete proteases and cellulases that hydrolyse complex organics, whereas Bacteroidota ferment the resulting monomers and strongly influence bulk pH [41]. Differences in performance between open-circuit and closed-circuit MFCs under identical conditions are primarily attributable to variations in the microbial composition of anode biofilms. Firmicutes and Proteobacteria, the predominant electrogenic taxa in MFC systems, exhibited combined relative abundances of 47.43% (S), 42.00% (C), 28.40% (SC), and 40.26% (SCC) in closed-circuit MFCs. These abundances were 57.53%, 51.41%, 20.40%, and 116.01% higher than those in corresponding open-circuit groups and 62.09%, 80.69%, −2.95%, and 2.72% higher than those in blank control groups. These results suggest that electron transfer in closed-circuit MFCs significantly shapes microbial community structure, enhancing the dominance of electrogenic bacteria and conferring greater resilience to environmental stressors, such as antibiotics, compared to MFC-0.

Single-antibiotic exposure stimulated overall biomass, yet dual antibiotics (SC) repressed *Firmicutes* and *Actinobacteriota* while favouring *Proteobacteria*, *Synergistota* and *Desulfobacterota* (e.g., *Desulfovibrio*). The addition of Cu^{2+} (SCC) partially reversed this shift, with Firmicutes recovering to a relative abundance of 30.56%, driven primarily by the heavy metal tolerance of genera such as *Trichococcus*. Throughout the trial, closed-circuit reactors contained markedly less Actinobacteriota and Chloroflexi than open-circuit units, consistent with their weak electrogenic potential and poor adaptation to an electrode-redox environment, aligning with findings by Lai et al. [42]. These findings highlight the critical influence of microbial community dynamics on MFC performance, particularly in response to antibiotics and heavy metal stressors. The enhanced electrogenic activity and microbial resilience in closed-circuit systems underscore their potential for bioenergy production and wastewater treatment under challenging environmental conditions.

3.2.2. Genus-level electrogenic and metal-resistance traits

As shown in Fig.3b, the key genera that shaped anodic biofilm function was highlighted, including *Trichococcus*, *Bacteroidetes_vadinHA17*, *Rhodococcus*, *JGI-0000079-D21*, *Sulfurovum*, *Caldisericum*, and *Brooklawnia*. The first three are recognised electro-active taxa whose cumulative relative abundances were 1.16-2.01-fold higher in closed-circuit MFCs than in open-circuit controls and 1.02-1.70-fold higher than in the blank (MFC-0), underscoring the selective pressure exerted by

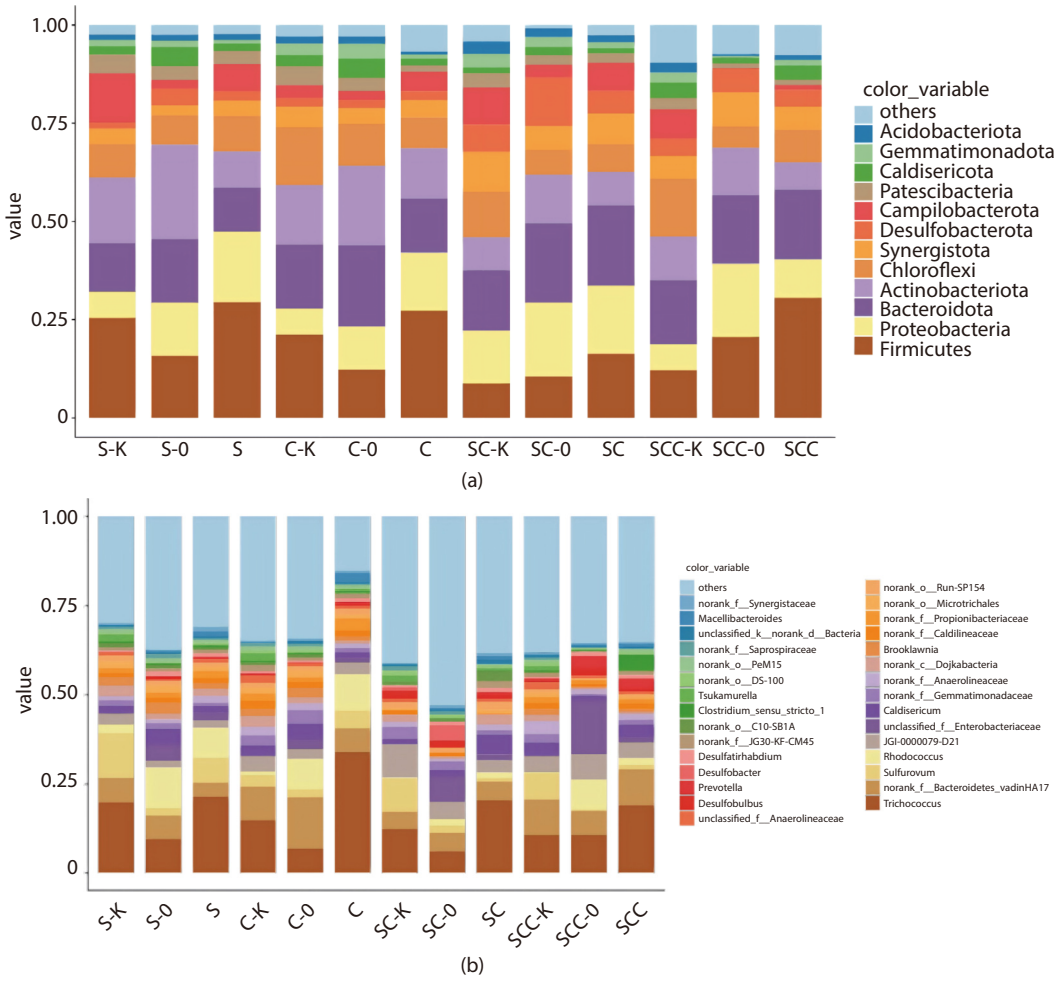

Fig. 3. Microbial community analysis at phylum level (a). Analysis of microbial communities at the genus level (b).

anodic electron transfer. *Trichococcus* maintained superior abundance across all phases, reflecting its intrinsic tolerance to both antibiotics and Cu^{2+} and its capacity to channel carbohydrate oxidation into current generation, thereby stabilising power output. *Bacteroidetes_vadinHA17* increased sharply upon Cu^{2+} addition. Its respiratory flexibility and ability to reduce electron carriers enable it to sustain fermentation and extracellular electron transfer under metal stress. *Rhodococcus*, a well-known Cu^{2+} biosorbent, mediated heavy-metal removal through surface complexation and intracellular accumulation, but its abundance declined in the SCC phase as cellular Cu burdens rose, indicating a trade-off between adsorption capacity and toxicity [30]. *JGI-0000079-D21* also responded positively to Cu^{2+}, yet attained higher levels in open-circuit reactors, implying that it contributes to metal resistance rather than electricity generation. Overall, the genus-level dynamics illustrate how closed-circuit operation simultaneously enriches electrogens and Cu-tolerant taxa, sustaining both reductive current production and metal removal even under co-stress conditio.

3.3. Resistance gene changes and dissemination mechanism.

3.3.1. Sulfonamide resistance genes

The removal of the chemical does not equate to a reduction in genetic risk, so the resistance genes were assayed. Sulfonamide resistance genes confer sulfonamide resistance by encoding dihydropteroate synthase enzymes that are insensitive to sulfonamide drugs, ensuring the production of dihydrofolic acid. Fig.4 shows that *sul-2* and *sul-3* rose sharply in the SMX-only phase (S), whereas *sul-1* peaked under combined antibiotics (SC). The further addition of Cu^{2+} (SCC) amplified all three genes, emphasising the co-selective effect of heavy-metal stress. The primary hosts of *sul* genes are *Trichococcus*, *norank_f__Propionibacteriaceae*, *norank_f__JG30-KF-CM45*, and *Macellibacteroides*, which are predominantly found in the phyla *Firmicutes*, *Actinobacteriota*, *Chloroflexi*, and *Bacteroidota*. In the CIP-only phase (C), the abundance of *Trichococcus* reached 33.89% due to its insensitivity to CIP, which grants it higher activity and environmental adaptability compared to other bacteria. In the SC phase, the abundance of *Trichococcus* sharply decreased to 5.54%, demonstrating the sensitivity of Gram-positive bacteria to SMX. This sensitivity is mainly attributed to the lack of complex membrane structures and a sufficient number of efflux pumps, which are more prevalent in Gram-negative bacteria [43]. The recovery of *Trichococcus* abundance in the SCC phase presumably attributed to horizontal acquisition of *sul-1* through *intI-1*-mediated gene cassettes. *Norank_f__Propionibacteriaceae* and *Macellibacteroides*, important propionic/acetic-acid producers that modulate pH through [44], were also positive predictors of *sul* abundance. Whereas, *norank_f__Saprospiraceae*, a key phosphorus-removing genus [45], showed a significant negative correlation with resistance genes, particularly *sul-2*, suggesting that phosphorus-removing conditions may indirectly suppress sulfonamide resistance.

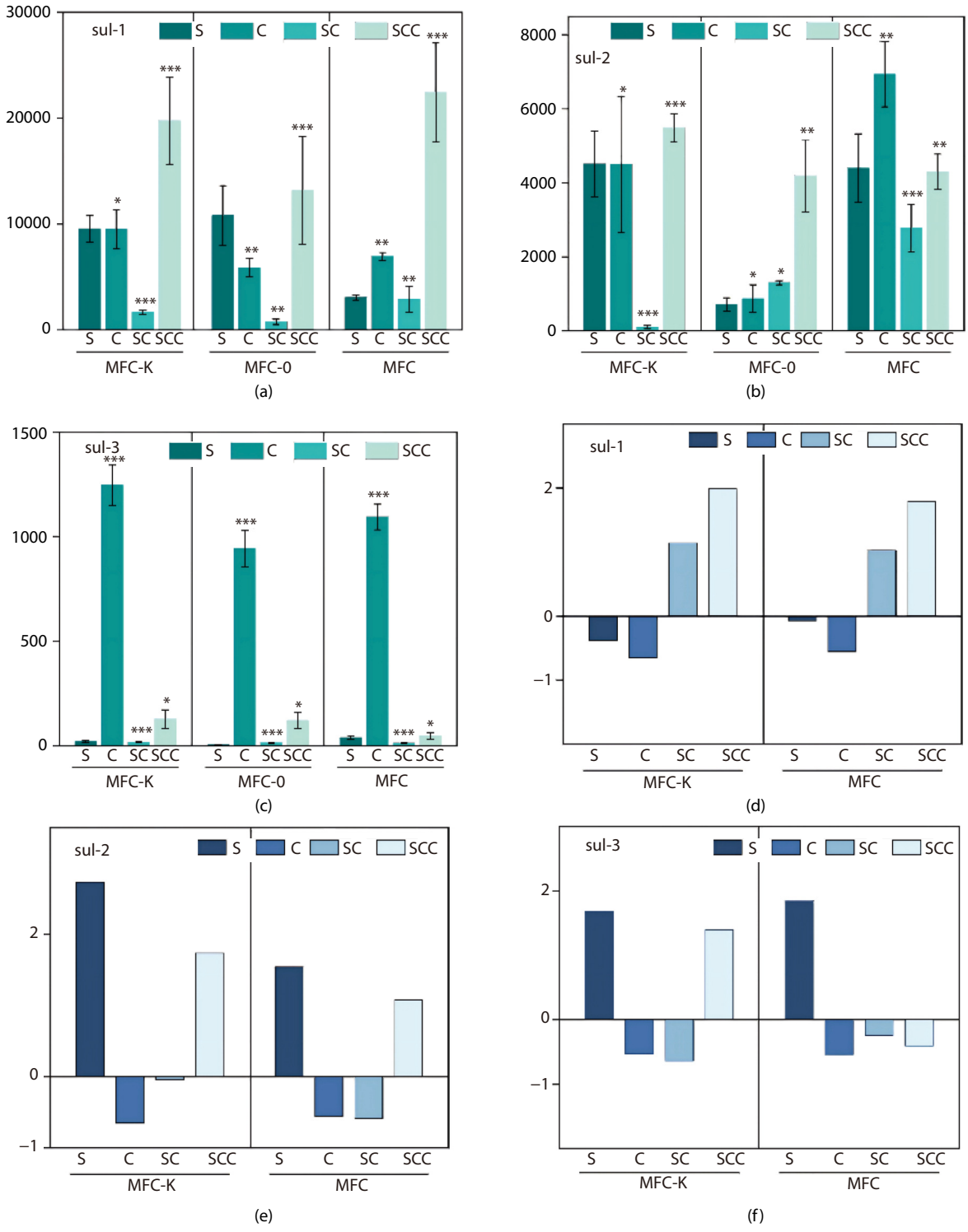

Fig. 4. Sulfonamide resistance gene abundance analysis. Absolute abundance: (a) *sul-1*; (b) *sul-2*; (c) *sul-3*; Relative Variation: (d) *sul-1*; (e) *sul-2*; (f) *sul-3*. (* p≤0.05 ** p≤0.01 *** p≤0.001)

3.3.2. Quinolone resistance genes

Quinolone resistance determinants (*qnr-A/D/S*, aac(6′)-Ib-cr) encode DNA-gyrase protectants or modifying enzymes. Closed-circuit MFCs exhibited significant up-regulation of *qnr-D*, *qnr-S* and aac(6′)-Ib-cr in SC and SCC phases, whereas open-circuit controls showed only minor fluctuations in *qnr-A* and aac(6′)-Ib-cr (Fig. 5). Core hosts included *Trichococcus*, *norank_f__Propionibacteriaceae*, *Clostridium_sensu_stricto*_1 and *Desulfatirhabdium*. *C. sensu_stricto*_1 increased from 0.16% to 4.2% after Cu^{2+} addition, paralleling the rise in *qnr-S* and *intI-1*, and confirming the metal-driven expansion of multi-resistant Firmicutes. Conversely, *norank_o__C10-SB1A* and *Caldisericum* proliferated in SC without harbouring major *qnr* genes, indicating alternative, possibly chromosomal, resistance mechanisms.

3.3.3. Horizontal gene transfer (HGT)

The Cu^{2+} not only co-selects for metal-resistance genes (MRGs) but also creates redox and osmotic stress that accelerate horizontal gene transfer. *Clostridium_sensu_stricto*_1 increased from 0.16% to 4.23% after Cu^{2+} addition and was tightly linked

to simultaneous rises in *qnr-S* and *intI-1* (Fig. 5). Its ability to form endospores and maintain metabolism under metal stress provides a stable intracellular niche for class 1 integrons, thereby promoting HGT between Firmicutes and neighbouring taxa. Conversely, *norank_o__C10-SB1A* proliferated in the SC phase (2.88%) without harbouring dominant ARGs, suggesting chromosomally encoded resistance or yet-uncharacterised defence systems worthy of further genomic exploration. *Caldisericota* member *Caldisericum* also expanded from 1.73% to 5.49%, mainly because its thermotolerant, low-pH optimum aligns with the Cu-acidified micro-environment. Closed-circuit operation intensified these effects. The *intI*-1 copy numbers increased 4.10-fold after Cu^{2+} addition, versus 1.87-fold in open-circuit controls (Fig. S9), confirming that anodic redox gradients and continuous hydraulic selection jointly enhance integron activity. Pearson co-occurrence analysis further revealed significant positive correlations between *qnr-D* and *sul-2*/*sul-3* ($\rho > 0.82$, $p < 0.01$) and between *cus-A* (Cu efflux) and *sul-3* ($\rho = 0.79$), implying that single plasmids or transposons encode both MRGs and ARGs. Consequently, Cu selection indirectly enriches sulfonamide resistance even in the absence of SMX.

To further evaluate whether HGT is enhanced during MFC

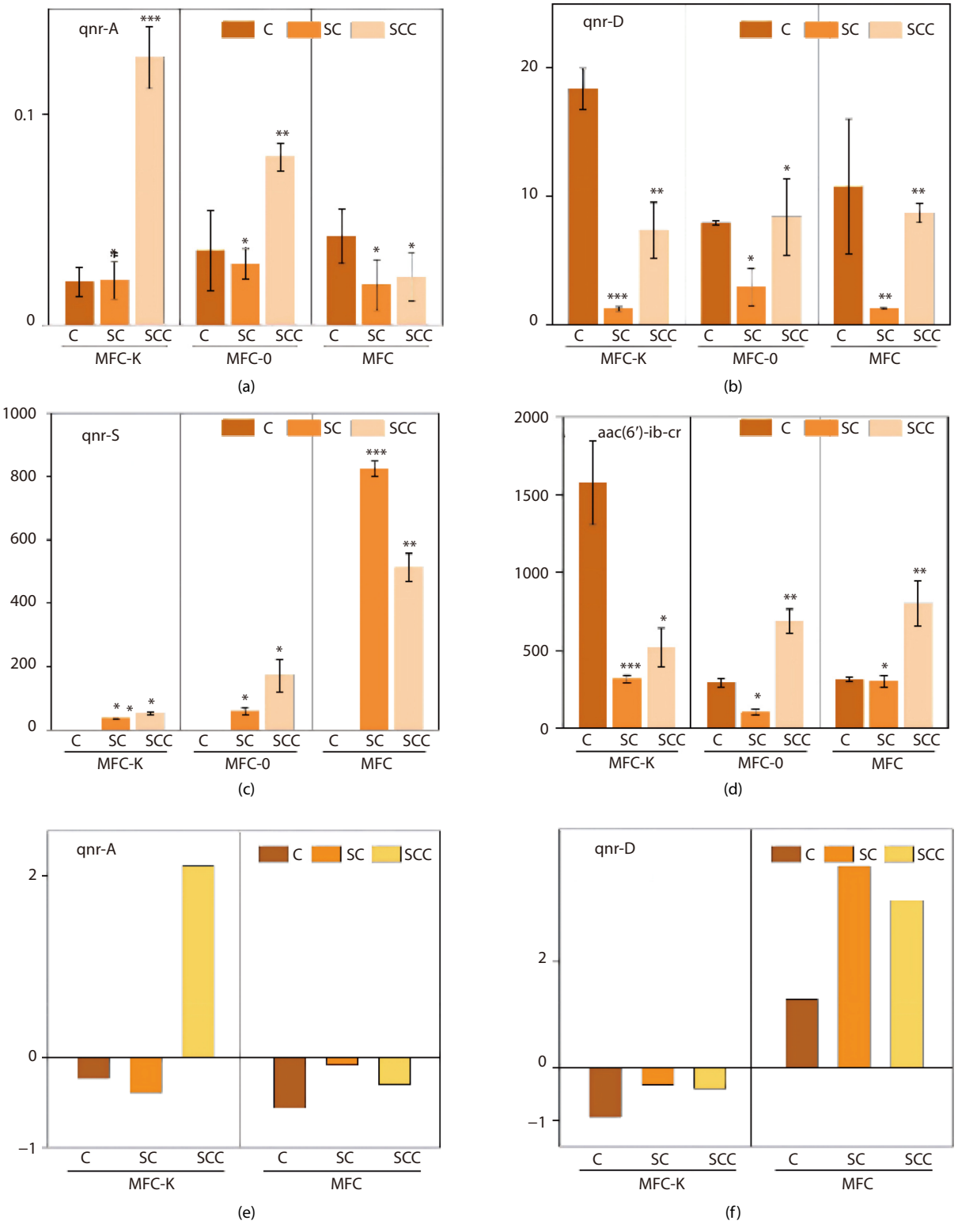

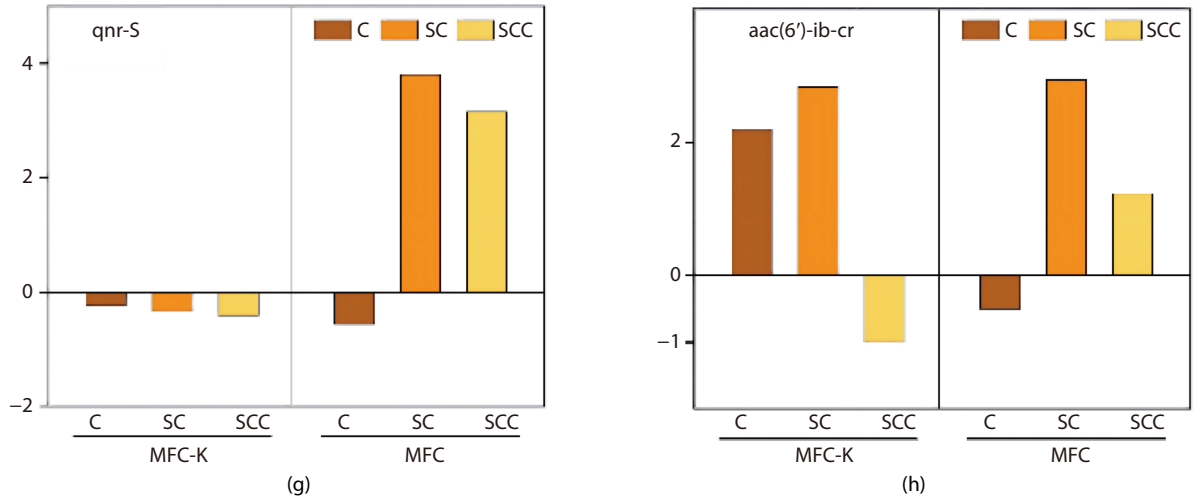

Fig. 5. Analysis of quinolone resistance gene abundance. Absolute abundance: (a). *qnr-A*; (b). *qnr-D*; (c). *qnr-S*; (d). *aac(6')-ib-cr*. Relative changes: (e). *qnr-A*; (f). *qnr-D*; (g). *qnr-S*; (h). *aac(6')-ib-cr*. (* p≤0.05 ** p≤0.01 *** p≤0.001)

operation, we compared the co-occurrence relationship between ARGs and MGEs before and after stable operation of the reactor. Pearson correlation analysis showed that the correlation between ARGs and intI-1 was weak or insignificant in the water intake and initial operation stages. However, under the condition of stable operation of closed circuit MFC, especially under the combined stress of antibiotics and Cu^{2+}, there was a significant positive correlation between intI-1 and ARGs, including sul-1, sul-2, sul-3, qnr-D and qnr-S ($\rho > 0.7$, $p < 0.01$).

This change suggests that MFC run promotes the colocalization of ARGs with MGEs in anodal biofilms, thereby enhancing horizontal gene transfer in an integron-mediated manner. The electrochemical polarization and Cu^{2+}-induced stress environment may accelerate the mobilization and spread of drug resistance genes by increasing the cell membrane permeability and recombination activity.

3.3.4. Correlation analysis between resistance genes and microorganisms

As shown in Fig. 6, *JGI-0000079-D21* and *Desulfovibrio* were positively correlated and associated with both *qnr-S* and *cop-A* genes. *Desulfovibrio*, a sulfate-reducing bacterium known to carry plasmid-borne metal clusters [46], may shuttle these determinants across Gram-negative recipients. In contrast, *norank_o_Microtichales*, *norank_o_PeM15*, *norank_f_Propionibacteriaceae*, and *Brooklawnia* were negatively correlated with *qnr-S* and *cop-A* genes, indicating sensitivity to combined antibiotic/Cu stress and a limited role in resistance propagation.

Multi-ARG hubs were also evident. *Trichococcus* abundance explained 87% of the variance in total *sul* gene copies, confirming its function as a keystone resistance reservoir. *Bacteroides_vadinHA17* was uniquely correlated with *intI-1* (ρ = 0.92), implicating it as an integron-mediated dissemination vector for *sul-1* and *sul-2* within the biofilm. Likewise, *norank_f__JG30-KF-CM45* displayed strong positive links to all three sulfonamide genes, underscoring its contribution to sulphonamide resistance proliferation.

Collectively, these findings demonstrate that Cu^{2+}-driven HGT, amplified by closed-circuit electrochemical conditions, creates a self-reinforcing cycle of ARG-MRG co-enrichment. From a health risk perspective, the potential pathogenicity of ARG hosts is of concern. The major ARG-related bacterial genera enriched in the MFC system, such as Trichococcus, Rhodococcus, Clostridium_sensu_stricto_1 and Bacteroidetes_vadinHA17) are usually classified as environmental or opportunistic pathogens rather than obligate pathogens. These genera are widely distributed in sewage treatment systems and natural anaerobic environments.

Despite its low intrinsic pathogenicity, its strong environmental adaptability, ability to form biofilms, and high frequency of association with mobile genetic elements suggest its potential existence as a gene pool for drug resistance. Under suitable conditions, these host-borne ARGs may still be transmitted to pathogenic bacteria through horizontal gene transfer, thus posing a potential public health risk. Although MFCs efficiently remove dissolved antibiotics and metals, they cannot inherently contain the genetic resistance reservoir; post-treatment barriers (e.g., UV, membrane filtration, or ARG-

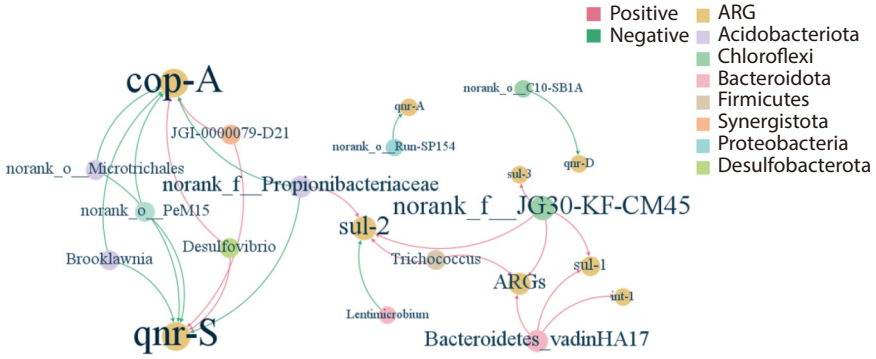

Fig. 6. Analysis of the correlation factors between resistance genes and microbial communities.

specific bacteriophages) are therefore essential to minimise downstream resistance dissemination.

3.4. Functional Prediction with PICRUSt2

3.4.1. KEGG Enzyme

Sulfamethoxazole competes with *p-aminobenzoate* for dihydropteroate synthase (DHFS). The *sul*-encoded isoform bypasses this inhibition. PICRUSt2 predicts a persistently higher DHFS abundance in closed-circuit MFCs (Fig. S10a), confirming that anodic conditions enrich *sul* genotypes even before SMX exposure. Concurrent predicted upregulation of dihydrofolate reductase (DHFR) under CIP stress may reflect increased one-carbon metabolism associated with DNA repair and cellular turnover, which is consistent with the higher overall metabolic activity measured in polarised biofilms. The *qnr* products sterically hinder drug binding [47]. Topoisomerase abundance was marginally higher in MFC biofilms, but the ratio of enzyme to *qnr* protection protein was lower than in open-circuit controls (Fig. S10b). Moderate electrical stimulation accelerates DNA turnover (higher polymerase activity) and shortens the window for quinolone binding, thereby reducing the selective advantage of *qnr* carriage and partially mitigating resistance-gene pollution. The bifunctional aminoglycoside acetyl-transferase AAC (6′)-Ib-cr also acetylates ciprofloxacin. PICRUSt2 prediction indicated an increased abundance of AAC(6′)-Ib-cr–related functions in CIP-only MFCs, whereas these functions were markedly reduced when Cu^{2+} was present (Fig. S10c). Combined antibiotic–metal stress likely destabilises the AAC (6′)-Ib fold or competes for acetyl-CoA, restoring drug sensitivity [48]. Thus, these results suggested that redox conditions within MFCs may modulate post-translational and genetic resistance mechanisms.

3.4.2. COG-based microbial function prediction analysis

PICRUSt2 profiling revealed that >55% of predicted proteins fall into three core COG categories: amino-acid transport & metabolism, translation & ribosomal structure, and energy production & conversion, regardless of additive (Fig. 7a). Pollutant stress shifted resources toward DNA replication, recombination & repair, transcription and cell-cycle control. These SOS-related functions were significantly more abundant in closed-circuit MFCs than in open-circuit controls, suggesting an active damage-repair response that enhances tolerance to antibiotics and Cu^{2+} [49]. Notably, enrichment of functions related to stress response and DNA repair may enhance the persistence of ARG hosts in adverse environments, thereby indirectly increasing the likelihood of ARG transmission to pathogenic bacteria in downstream environments. The concomitant decline in category C is consistent with the measured decrease in coulombic efficiency and COD removal during SC/SCC stages, suggesting that energy may be diverted from current generation to cellular defence. Stage-by-stage comparison (Fig. S11) shows that heavy-metal was associated with elevated two functional subsets: 1) Cell repair & carbohydrate metabolism - required for Cu-chelation and EPS synthesis; and 2) Efflux & trafficking systems - including type-IV secretion and retro-transposon-associated COGs that are involved in integron mobilization. All increases were significantly significantly larger in MFCs than in open-circuit reactors, demonstrating that anodic polarization may amplify functional expression under medium pollutant load. The same trend is consistent with the higher *qnr* and *intI-1* copy numbers in MFCs: DNA-replication-linked resistance genes may benefit from the elevated polymerase activity needed for rapid biomass turnover.

Cu-specific defence is not restricted to efflux pumps. Fig. 7b and Fig. S12 highlight a pronounced rise in P-type ATPase Cu-transporters (COG 2217, *copA-like*). ATP-driven conformational pumping is considered a dominant detoxification route in Rhodococcus and other anode-enriched taxa [50]. Because

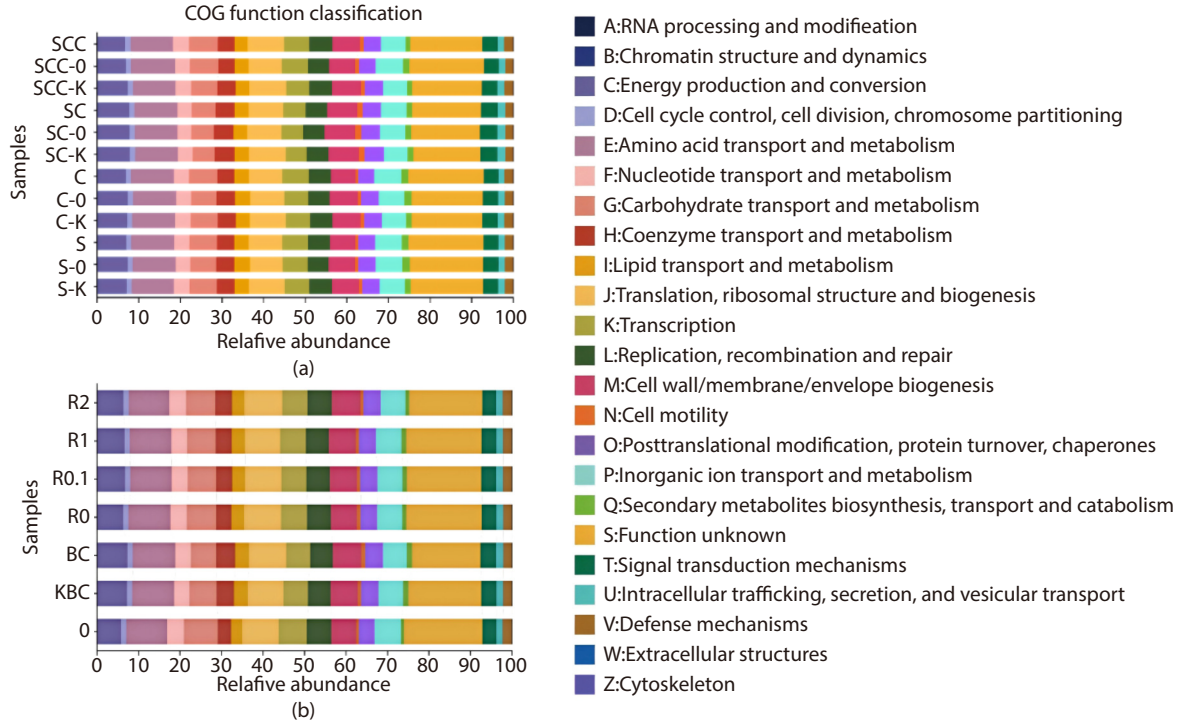

Fig. 7. (a) Changes in relative abundance of COG function in different samples (b) The Changes in relative abundance of COG function under the influence of Cu^{2+}.

closed-circuit reactors are associated with higher proton-motive force and ATP turnover, the energetic cost of Cu export may be more readily met, which is consistent with both the superior metal-removal efficiency and the potential co-selection of ARGs that share the same plasmid backbone. Thus, the MFC environment may enhance microbial adaptability, but the energetic advantage that underpins higher current may also support efflux pumps and integron machinery, suggesting a trade-off between treatment performance and resistance control [51].

4. Conclusion

This study evaluated the performance and ARG dynamics of MFCs treating swine wastewater under co-exposure to SMX, CIP and Cu^{2+}. It included that closed-circuit MFCs maintained COD, SMX and CIP removals at >90%, >95% and >99%, respectively, outperforming open-circuit controls. Despite a drop in coulombic efficiency under Cu^{2+} addition, stable electricity generation confirmed strong adaptability to complex contamination of MFC. Electrochemical selection enriched electro-active and Cu-tolerant taxa, conferring rapid self-repair and functional stability under antibiotic-metal co-stress. The presence of Cu^{2+} increased the abundance of class-1 integrons and the copy numbers of *sul*, *qnr* and *cus* genes via co-selection and HGT. Efficient antibiotic degradation did not curtail ARGs, instead, an electrode-bound resistance reservoir was established. The PICRUSt2 analysis suggested that that closed-circuit operation was associated with enhanced DNA repair, heavy-metal efflux and integrase-related functions, which may providing metabolic and energetic support for ARG maintenance and dissemination. Thus, MFCs under combined antibiotic–metal stress may promote ARG persistence without post-treatment barriers.

Acknowledgments

This research was supported by National Natural Science Foundation of China (No. 52300210); Shandong Excellent Youth Science Fund Project (Overseas) (2023HWYQ-077); The Taishan scholars Program of Shandong Province (tsqn202211157); and Project of Shandong Province Higher Educational Young Innovative Talent Introduction and Cultivation Team [Wastewater Treatment and Resource Innovation Team] (ZXQT20211216001).

Conflicts of Interest:

The authors declare that they have no known competing financial interests or personal relationships that could have appeared to influence the work reported in this paper.

CRediT author contributions

Weidong Shang: Writing–review & editing, Writing–origi-nal draft, Funding acquisition, Formal analysis, Data curation, Conceptualization. Yufei Liu: Writing–review & editing, Methodology, For-mal analysis, Conceptualization. Dongle Cheng: Writing–review & editing, Visualization, Conceptualization. Huaqing Liu: Supervision, Software, Concep-tualization. Huu Hao Ngo: Methodology, Investigation, Conceptualiza-tion. Wenshan Guo: Visualization, Project administration, Con-ceptualization. Lin Li: Validation, Supervision, Resources. Xinhan Chen: Resources, Investigation.

Data Availability

All data needed to support the conclusions in the paper are presented in the manuscript and/or the Supplementary Materials. Additional data related to this paper may be requested from the corresponding author upon request.

Electronic Supplementary Material (ESM)

The online version contains supplementary material available at https://doi.org/10.26599/ECS.2026.9600008.

References

[1] Li, N.; Chen, J. G.; Liu, C.; Yang, J. X.; Zhu, C. X.; Li, H. N. Cu and Zn exert a greater influence on antibiotic resistance and its transfer than doxycycline in agricultural soils. *J. Hazard. Mater.*, 2022, 423: 127042.

[2] Wei, H. D.; Wu, X.; Chen, A. X.; Liu, K. Y.; Lv, Z.; Qi, T. L.; Lu, Y.; Tao, Y.; Liu, C. Y. Reserve and proliferation characteristics of antibiotic resistance genes and heavy metal resistance genes in the sewage pipe biofilm under the stress of Cu and Zn. *J. Environ. Chem. Eng.*, 2025, 13: 116162.

[3] Li, H. K.; Shen, M. C.; Li, M. Y.; Tao, S. Y.; Li, T. H.; Yang, Z. X. Removal of microplastics and resistance genes in livestock and aquaculture wastewater: Current knowledge and future directions. *J. Environ. Chem. Eng.*, 2024, 12: 113384.

[4] Tella, M.; Legros, S.; Monteiro, A. N. T. R., Forouzandeh, A.; Penen, F.; Durosoy, S.; Doelsch, E. Unexpected Cu and Zn speciation patterns in the broiler feed-animal-excreta system revealed by XAS spectroscopy. *Chemosphere*, 2023, 340: 139684.

[5] Wang, X. R.; Zhang, X.; Li, N.; Yang, Z. Z.; Li, B. X.; Zhang, X. L.; Li, H. N. Prioritized regional management for antibiotics and heavy metals in animal manure across China. *J. Hazard. Mater.*, 2024, 461: 132706.

[6] Feng, Z. M.; Zhu, H. H.; Deng, Q. F.; He, Y. M.; Li, J.; Yin, J.; Gao, F. X.; Huang, R. L.; Li, T. J. Environmental pollution induced by heavy metal(loid)s from pig farming. *Environ. Earth Sci.*, 2018, 77: 103.

[7] Gonzalez Ronquillo, M.; Angeles Hernandez, J. C. Antibiotic and synthetic growth promoters in animal diets: Review of impact and analytical methods. *Food Control*, 2017, 72: 255–267.

[8] Wilson, B.; Pyatt, F. B. Heavy metal bioaccumulation by the important food plant, olea europaea L., in an ancient metalliferous polluted area of Cyprus. *Bull. Environ. Contam. Toxicol.*, 2007, 78: 390–394.

[9] Zeng, S. Q.; He, Y.; Li, X. Q.; Li, Y.; Tian, H. L.; Yin, R. P.; Zhang, Q. H.; Yu, D. Y. The livestock and poultry farming impact on antibiotic pollution in China and the potential of nitrogen-doped biochar for remediation. *J. Environ. Manag.*, 2025, 383: 125462.

[10] Ben, W. W.; Pan, X.; Qiang, Z. M. Occurrence and partition of antibiotics in the liquid and solid phases of swine wastewater from concentrated animal feeding operations in Shandong Province, China. *Environ. Sci.: Processes Impacts*, 2013, 15: 870.

[11] de Sousa Oliveira, A. P., Assemany, P.; Covell, L.; Calijuri, M. L. Copper multifaceted interferences during swine wastewater treatment in high-rate algal ponds: Alterations on nutrient removal, biomass composition and resource recovery. *Environ. Pollut.*, 2023, 324: 121364.

[12] Guo, X. R.; Qi, Z.; Li, J. S.; Tong, H. L.; Ren, N. Q.; You, S. J. Overlooked volcanic effect during transmission of antibiotic resistance genes induced by copper and zinc. *Chemosphere*, 2024, 362: 142713.

[13] Fan, Z. Z.; Du, Y. W.; Zhang, J. L.; Yang, X. P. Pathogenic bacteria and high-risk ARGs removal in subsurface flow constructed wetlands treating swine tailwater: Performance and influencing

factors. *Chem. Eng. J.*, 2025, 507: 160582.
[14] Hu, T.; Hao, Q. Q.; Qian, X.; Yan, G. F.; Gu, J.; Sun, W. Normal levels of Cu and Zn contamination present in swine manure increase the antibiotic resistance gene abundances in composting products. *Process. Saf. Environ. Prot.*, 2025, 194: 402–411.
[15] Li, T.; Li, C. Y.; Wang, Y. F.; Zhang, J. N.; Li, H.; Wu, H. F.; Yang, X. L.; Song, H. L. Insights to the cooperation of double-working potential electroactive biofilm for performance of sulfamethoxazole removal: ARG fate and microorganism communities. *J. Hazard. Mater.*, 2024, 477: 135357.
[16] Liang, L. Y.; Lin, Y. Z.; Ren, R. J.; Zhang, Q. J.; Qu, J. Q.; Liu, Y. H.; Han, Z.; Sun, X. Recent advances in antibiotic removal using independent and coupled microbial fuel cells (MFCs): Mechanisms and cells (MFCs): Mechanisms and practical applications. *J. Water Process. Eng.*, 2025, 71: 107226.
[17] Zhao, X. D.; Qiao, Q. Q.; Qin, X. R.; Zhao, P. Y.; Li, X. J.; Xie, J.; Zhai, F. H.; Li, Y. T. Viral community and antibiotic resistance genes carried by virus in soil microbial fuel cells. *Sci. Total Environ.*, 2024, 955: 177260.
[18] Li, H.; Cao, H. P.; Li, T.; He, Z. M.; Zhao, J. H.; Zhang, Y. F.; Song, H. L. Biofilm electrode reactor coupled manganese ore substrate upflow microbial fuel cell-constructed wetland system: High removal efficiencies of antibiotic, zinc (II), and the corresponding antibiotic resistance genes. *J. Hazard. Mater.*, 2023, 460: 132394.
[19] Castellano-Hinojosa, A.; Gallardo-Altamirano, M. J.; Pozo, C.; González-Martínez, A.; González-López, J. Hydraulic retention time drives changes in energy production and the anodic microbiome of a microbial fuel cell (MFC). *J. Water Process. Eng.*, 2024, 59: 104966.
[20] Chen, N. W.; Zhang, X. B.; Du, Q.; Huo, J. B.; Wang, H. Z.; Wang, Z. W.; Guo, W. S.; Ngo, H. H. Advancements in swine wastewater treatment: Removal mechanisms, influential factors, and optimization strategies. *J. Water Process. Eng.*, 2023, 54: 103986.
[21] Guo, J. Y.; Li, Q. H.; Gao, Q. F.; Shen, F.; Yang, Y. T.; Zhang, X. Y.; Luo, H. Comparative study on the treatment of swine wastewater by VFCW-MFC and VFCW: Pollutants removal, electricity generation, microorganism community. *J. Environ. Manag.*, 2023, 342: 118299.
[22] Wang, J. L.; Chen, X. Y. Removal of antibiotic resistance genes (ARGs) in various wastewater treatment processes: An overview. *Crit. Rev. Environ. Sci. Technol.*, 2022, 52: 571–630.
[23] Yin, X. F.; Liu, L. X.; Shao, W.; Ai, M.; Liang, G. B. High-performance bacterium-enhanced dual-compartment microbial fuel cells for simultaneous treatment of food waste oil and copper-containing wastewater. *Sci. Rep.*, 2024, 14: 23244.
[24] Liu, Y. F.; Zhang, J.; Cheng, D. L.; Guo, W. S.; Liu, X. Q.; Chen, Z. J.; Zhang, Z. H.; Ngo, H. H. Fate and mitigation of antibiotics and antibiotic resistance genes in microbial fuel cell and coupled systems. *Sci. Total Environ.*, 2024, 938: 173530.
[25] Yan, W. F.; Guo, Y. Y.; Xiao, Y.; Wang, S. H.; Ding, R.; Jiang, J. Q.; Gang, H. Y.; Wang, H.; Yang, J.; Zhao, F. The changes of bacterial communities and antibiotic resistance genes in microbial fuel cells during long-term oxytetracycline processing. *Water Res.*, 2018, 142: 105–114.
[26] Ma, X. F.; Guo, N.; Ren, S. J.; Wang, S. G.; Wang, Y. K. Response of antibiotic resistance to the co-existence of chloramphenicol and copper during bio-electrochemical treatment of antibiotic-containing wastewater. *Environ. Int.*, 2019, 126: 127–133.
[27] Mallick, S.; Pradhan, T.; Das, S. Bacterial biomineralization of heavy metals and its influencing factors for metal bioremediation. *J. Environ. Manag.*, 2025, 373: 123977.
[28] Li, M.; Zhou, S. Q. Efficacy of Cu(II) as an electron-shuttle mediator for improved bioelectricity generation and Cr(VI) reduction in microbial fuel cells. *Bioresour. Technol.*, 2019, 273: 122–129.
[29] Wang, N.; Peng, L.; Gu, Y.; Liang, C. Z.; Pott, R. W. M., Xu, Y. F. Insights into biodegradation of antibiotics during the biofilm-based wastewater treatment processes. *J. Clean. Prod.*, 2023, 393: 136321.
[30] Nazari, M. T., Simon, V.; Machado, B. S., Crestani, L.; Marchezi, G.; Concolato, G.; Ferrari, V.; Colla, L. M., Piccin, J. S. Rhodococcus: A promising genus of actinomycetes for the bioremediation of organic and inorganic contaminants. *J. Environ. Manag.*, 2022, 323: 116220.
[31] Shi, W. C.; He, Z. M.; Lu, J. H.; Wang, L. F.; Guo, J. H.; Qiu, S.; Ge, S. J. Response of nitrifiers to gradually increasing pH conditions in a membrane nitrification bioreactor: Microbial dynamics and alkali-resistant mechanism. *Water Res.*, 2025, 268: 122567.
[32] Tang, T. T.; Liu, M.; Du, Y.; Chen, Y. Deciphering the internal mechanisms of ciprofloxacin affected anaerobic digestion, its degradation and detoxification mechanism. *Sci. Total Environ.*, 2022, 842: 156718.
[33] Trueba-Santiso, A.; Rivadulla, M.; Casabella-Font, O.; Cuervo-Lumbaque, E.; Radjenovic, J.; Omil, F.; Suárez, S. Ciprofloxacin biotransformation during anaerobic digestion: Major transformation products elucidation and environmental proteomics. *J. Hazard. Mater.*, 2025, 495: 139159.
[34] Akay, C.; Ulrich, N.; Rocha, U.; Ding, C.; Adrian, L. Sequential anaerobic–aerobic treatment enhances sulfamethoxazole removal: From batch cultures to observations in a large-scale wastewater treatment plant. *Environ. Sci. Technol.*, 2024, 58: 12609–12620.
[35] Liu, J. W.; Yang, X. Y.; Gao, T.; Zhang, Y. H.; Pan, D. D.; He, J.; Wu, X. W. Revealing the anaerobic biodegradation pathway and mechanism of sulfamethoxazole by a novel Cupidesulfovibrio sp. strain SA-9. *Water Res.*, 2026, 290: 125118.
[36] Wang, R.; Chen, J. P.; Chen, H. Y. Performance and mechanism of antibiotic resistance removal by biochar-enhanced sediment microbial fuel cell. *Bioresour. Technol.*, 2024, 412: 131371.
[37] Mei, R.; Nobu, M. K.; Narihiro, T.; Liu, W. T. Metagenomic and metatranscriptomic analyses revealed uncultured bacteroidales populations as the dominant proteolytic amino acid degraders in anaerobic digesters. *Front. Microbiol.*, 2020, 11: 593006.
[38] Xu, C. L.; Feng, Y. L.; Li, H. R.; Wu, R. F.; Ju, J. R.; Liu, S. L.; Yang, Y.; Wang, B. Adsorption of heavy metal ions by iron tailings: Behavior, mechanism, evaluation and new perspectives. *J. Clean. Prod.*, 2022, 344: 131065.
[39] Zhao, C. F.; Meng, S. Y.; Yan, L. G.; Zhang, X. W.; Wei, Q.; Wei, D. Coupling of submersible microbial fuel cell into aerobic granular sludge bioreactor for ciprofloxacin stress alleviation: Performance and mechanism. *J. Clean. Prod.*, 2022, 373: 133902.
[40] Zhao, C. F.; Wei, D.; Fan, D. W.; Meng, S. Y.; Bian, S. Y.; Zhang, X. W.; Du, B.; Wei, Q. Coupling of nitrifying granular sludge into microbial fuel cell system for wastewater treatment: System performance, electricity production and microbial community shift. *Bioresour. Technol.*, 2021, 326: 124741.
[41] Wang, R. M.; Li, C. X.; Lv, N.; Pan, X. F.; Cai, G. J.; Ning, J.; Zhu, G. F. Deeper insights into effect of activated carbon and nano-zerovalent iron addition on acidogenesis and whole anaerobic digestion. *Bioresour. Technol.*, 2021, 324: 124671.
[42] Lai, M. Y.; Hong, J. T.; Xu, X. L.; Li, Y. Y.; Liu, C. Y.; Jia, J. B.; Luan, T. G. The effect of inoculum source of different pollution levels on the performances of microbial fuel cell biosensors. *Sens. Actuat. B Chem.*, 2025, 422: 136614.
[43] Li, X. Z.; Plésiat, P.; Nikaido, H. The challenge of efflux-mediated antibiotic resistance in gram-negative bacteria. *Clin. Microbiol. Rev.*, 2015, 28: 337–418.
[44] Liu, T.; Zuo, J. E.; Shen, Z. Q.; Zhou, Y. X. Inhibition of biological acidification and mechanism of crotonaldehyde removal with glucose cometabolism. *J. Environ. Manag.*, 2022, 303: 114090.
[45] Jin, Z.; Ji, F. Y.; Xu, X.; Xu, X. Y.; Chen, Q. K.; Li, Q. Microbial and metabolic characterization of a denitrifying phosphorus-uptake/

side stream phosphorus removal system for treating domestic sewage. *Biodegradation*, 2014, 25: 777–786.

[46] Karnachuk, O. V., Beletsky, A. V., Rakitin, A. L., Ikkert, O. P., Avakyan, M. R., Zyusman, V. S., Napilov, A.; Mardanov, A. V., Ravin, N. V. Antibiotic-resistant desulfovibrio produces H_2S from supplements for animal farming. *Microorganisms*, 2023, 11: 838.

[47] Hooper, D. C.; Jacoby, G. A. Mechanisms of drug resistance: Quinolone resistance. *Ann. N Y Acad. Sci.*, 2015, 1354: 12–31.

[48] Reeves, C. M.; Magallon, J.; Rocha, K.; Tran, T.; Phan, K.; Vu, P.; Yi, Y.; Oakley-Havens, C. L.; Cedano, J.; Jimenez, V. et al. Aminoglycoside 6′-N-acetyltransferase type ib [AAC(6′)-ib]-mediated aminoglycoside resistance: Phenotypic conversion to susceptibility by silver ions. *Antibiotics*, 2021, 10: 29.

[49] Pu, Y. H.; Hao, Y. M.; Zeng, Q. Z.; Yang, Q.; Yang, B. W.; Wu, Y. X.; Yang, X. Y.; Sun, Y.; Wang, X.; Ma, Y. L. et al. Effects of UV-aged tire wear particles (TWPs) on soil microorganisms: Microbial community, microbial metabolism, cell defense and repair, and transmission of ARGs. *J. Environ. Chem. Eng.*, 2025, 13: 115624.

[50] Dmitriev, O. Y., Patry, J. Structure and mechanism of the human copper transporting ATPases: Fitting the pieces into a moving puzzle. *Biochim. Biophys. Acta BBA Biomembr.*, 2024, 1866: 184306.

[51] Li, Y. H.; Ma, J. H.; Wang, R.; Luo, Y.; Zheng, S. D.; Wang, X. D. Zinc transporter 1 functions in copper uptake and cuproptosis. *Cell Metab.*, 2024, 36: 2118–2129.e6.